Chinese Journal of Polymer Science Vol. 31, No. 12, (2013), 1670−1684

Chinese Journal of Polymer Science

MODIFICATION OF SODIUM SALT OF PARTIALLY CARBOXYMETHYLATED TAMARIND KERNEL POWDER THROUGH GRAFTING WITH ACRYLONITRILE: SYNTHESIS, CHARACTERIZATION AND SWELLING BEHAVIOR

J.H. Trivedi[a*], J.R. Jivani[b], K.H. Patel[a] and H.C. Trivedi[a]
[a] *P.G. Dept. of Chemistry, Sardar Patel University, Vallabh Vidyanagar, Gujarat State, India*
[b] *Amneal Phamaceuticals, New York, USA*

Abstract A graft copolymer of polyacrylonitrile (PAN) with sodium salt of partially carboxymethylated tamarind kernel powder (Na-PCMTKP, $\overline{DS}$ = 0.15) was synthesized by using ceric ammonium nitrate (CAN) as a redox initiator in an aqueous medium. The optimum reaction conditions for affording maximum percentage of grafting were established by successively varying reaction conditions such as concentrations of nitric acid, CAN, monomer (AN) as well as reaction time, temperature and amount of substrate. The influence of these reaction conditions on the grafting yields was discussed. The kinetic scheme of free radical graft copolymerization was proposed and the experimental results were found to agree very well with the proposed kinetic scheme. The graft copolymer (Na-PCMTKP-*g*-PAN, percentage of grafting G = 413.76% and percentage of grafting efficiency GE = 96.48%) sample synthesized under the established optimized reaction conditions was hydrolyzed by 0.7 mol·L^{-1} NaOH solution at 90–95 °C to yield the superabsorbent hydrogel, H-Na-PCMTKP-*g*-PAN. The swelling behavior of the hydrogel was studied by carrying out its absorbency measurements in low conductivity water, 0.15 mol·L^{-1} salt (NaCl, $CaCl_2$ and $AlCl_3$) solutions and simulated urine (SU) solution at different timings. FTIR, TGA and SEM techniques were used to characterize the products.

Keywords: Sodium salt of partially carboxymethylated tamarind kernel powder; Acrylonitrile; Graft copolymerization; Superabsorbent hydrogels; Swelling behavior.

INTRODUCTION

The chemical modification of natural, renewable polymers by grafting has received considerable attention in recent years as it functionalizes the natural, biopolymers to their potential, imparting desirable properties onto them without affecting the architecture of the polymer backbone[1]. Among commonly used types of hydrogels, natural based and especially polysaccharides based superabsorbent hydrogels exhibit potential applications in many fields such as hygienic products, agriculture and horticulture, pharmaceutics and medical applications[2, 3]. Graft copolymerization of vinyl monomers onto polysaccharides followed by crosslinking of their chains is regarded as an efficient method for the synthesis of polysaccharide based superabsorbent hydrogels[4–10].

Tamarind kernel powder (TKP), a food grade natural polysaccharide and one of the cheapest gums, is derived from the seeds of *Tamarindus indica Linn*; a common and most important tree of India and South East Asia. The polysaccharide is composed of D-galactose, D-xylose and D-glucose in the molar ratio of 1:2:3[11]. It consists of a main chain of β-D-(1→4) linked glucopyranosyl units, and a side chain consisting of a single xylopyranosyl unit is attached to every second, third and fourth D-glucopyranosyl units through an α-D-(1→6)

* Corresponding author: J.H. Trivedi, E-mail: drjignesh2575@yahoo.co.in
Received January 4, 2013; Revised March 2, 2013; Accepted March 12, 2013
doi: 10.1007/s10118-013-1366-9

linkage. One D-galactopyranosyl unit is attached to one of the xylopyranosyl units through a β-D-(1→2) linkage. TKP has potential commercial applications in textile, explosives, plywood and food industries. Even though TKP finds wide range of industrial applications, it also suffers from some drawbacks like biodegradability[12], which limits its uses considerably. These drawbacks can be improved through the grafting of vinyl monomers onto it. However, due to the low solubility of TKP in cold water, poor solution clarity as well as the desire for products with modified or special properties, we have used carboxymethylated derivative of tamarind kernel powder *i.e.* sodium salt of partially carboxymethylated tamarind kernel powder (Na-PCMTKP) in the present work for its further modification *via* grafting. Recently, graft copolymerization of acrylamide[13] as well as acrylonitrile[14] onto TKP using CAN as a redox initiator has been reported. The synthesis of carboxymethyl tamarind-*g*-acrylamide and its application as a novel polymeric flocculant has also been reported[15].

The comprehensive literature survey reveals that there is no published report regarding the modification of sodium salt of partially carboxymethylated tamarind kernel powder (Na-PCMTKP) by following the grafting technique. Recently, therefore, as a part of our research programme we have successfully carried out modification of Na-PCMTKP ($\overline{DS}$ = 0.15) by graft copolymerization with acrylonitrile (AN), methyl acrylate (MA), methyl methacrylate (MMA) and butyl acrylate (BA) using ceric ammonium nitrate (CAN) as a redox initiator. However, in the present work we report the evaluation of the optimal reaction conditions for affording maximum percentage of grafting of AN onto Na-PCMTKP ($\overline{DS}$ = 0.15) and the saponification of the optimally synthesized graft copolymer (Na-PCMTKP-*g*-PAN, G = 413.76%) to form a superabsorbent hydrogel, H-Na-PCMTKP-*g*-PAN. The swelling behavior of the hydrogel has also been studied in low conductivity water as well as in different saline solutions.

EXPERIMENTAL

Materials

Sodium salt of partially carboxymethylated tamarind kernel powder (Na-PCMTKP, $\overline{DS}$ = 0.15) was kindly supplied by Encore Natural Pvt. Ltd., Naroda, Ahmedabad (Gujarat, India). AN (Samir Tech. Pvt. Ltd., Baroda, Gujarat, India) was distilled out at atmospheric pressure, and the middle fraction was collected and used. CAN of reagent grade and analar grade nitric acid (both Qualigens India Ltd.) were used as received. Fresh solutions of the initiator were used, prepared by dissolving the required amount of CAN in nitric acid. Sodium hydroxide, calcium chloride and magnesium sulphate (all Samir Tech. Pvt. Ltd., Baroda, Gujarat, India) were used as received. Sodium chloride and urea (both Maruti Chemicals Corporation, Anand, Gujarat, India) as well as aluminum chloride (Loba Chemie, Mumbai, India) of analytical reagent grade were used as received. All other reagents and solvents used in the present work were of reagent grade. Nitrogen gas was purified by passing through fresh pyrogallol solution. Low conductivity water was used for the preparation of solutions as well as for polymerization reactions.

Graft Copolymerization

A 500 mL three-necked flask equipped with mechanical stirrer, a reflux condenser and a glass inlet system was immersed in a constant temperature bath for grafting reactions. In a typical reaction, varying amount of (0.5 to 3 g) of Na-PCMTKP ($\overline{DS}$ = 0.15) was dissolved in low conductivity water (100 mL) with constant stirring and bubbling a slow stream of nitrogen for 1 h at desired temperature (15 °C to 55 °C). Freshly prepared 10 mL solution of CAN (2.5×10^{-3} mol·L^{-1} to 80×10^{-3} mol·L^{-1}) in nitric acid (nil to 1.0 mol·L^{-1}) was added and stirred for 20 min. Nitrogen gas was continuously passed through the reaction solution and freshly distilled AN (0.037–0.370 mol·L^{-1}) was added. The grafting reactions were carried out for varying time intervals (0.5–10 h). After completion of the reaction, the mixture was immediately poured into excess of methanol to coagulate the crude graft copolymer. The crude graft copolymer product was filtered, repeatedly washed with nitric acid as well as 95% methanol and finally washed with pure methanol. The crude graft copolymer thus obtained was dried under vacuum at 40 °C. The homopolymer (PAN) was separated from the crude graft copolymer by extraction with dimethyl formamide for 48 h. After complete removal of the homopolymer, the pure graft copolymer was dried at 40 °C under vacuum to a constant weight.

The percentage of grafting G (%), percentage of grafting efficiency GE (%), percentage of homopolymer H_p (%) as well as rates of polymerization R_p and graft copolymerization R_g were evaluated by using the following expressions[16]:

$$G(\%) = \frac{\text{wt. of polymer grafted}}{\text{Initial wt. of backbone}} \times 100 \tag{1}$$

$$GE(\%) = \frac{\text{wt. of polymer grafted}}{\text{wt. of polymer grafted + wt. of homopolymer}} \times 100 \tag{2}$$

$$H_p(\%) = 100 - GE(\%) \tag{3}$$

$$R_p(\text{mol} \cdot \text{L}^{-1} \cdot \text{s}^{-1}) = \frac{\text{weight of polymer grafted + weight of homopolymer}}{\text{mol. wt. of monomer} \times \text{reaction time (s)} \times \text{volume of the reaction mix. (mL)}} \times 10^3 \tag{4}$$

$$R_p(\text{mol} \cdot \text{L}^{-1} \cdot \text{s}^{-1}) = \frac{\text{weight of polymer grafted}}{\text{mol. wt. of monomer} \times \text{reaction time (s)} \times \text{volume of the reaction mix. (mL)}} \times 10^3 \tag{5}$$

Isolation of Grafted Chains

The graft copolymer of Na-PCMTKP ($\overline{\text{DS}} = 0.15$) containing PAN (*i.e.* Na-PCMTKP-*g*-PAN) was hydrolyzed by refluxing it for 12 h in 1 mol·L^{-1} HCl as suggested by Brockway[17] for the isolation of the grafted PAN chains.

Saponification of Alkaline Hydrolysis of Graft Copolymer

The graft copolymer, Na-PCMTKP-*g*-PAN (G = 413.76%) synthesized under optimal reaction conditions, was saponified by following the methanol precipitate method[18] for the formation of hydrogel, H-Na-PCMTKP-*g*-PAN. According to this method, in a loosely stoppered 500 mL flask, 10.0 g of the Na-PCMTKP-*g*-PAN was dispersed in 100 mL 0.7 mol/L sodium hydroxide solution and gently stirred in the base under atmospheric conditions (5 mins). Then the dispersion was heated at 90–95 °C with occasional stirring. The saponification was continued until the color of the mixture changed from deep orange-red to light yellow (*ca.* 2.5 h). The pasty mixture was then allowed to cool to room temperature. Methanol (5 × 10 mL) was added portion-wise to the gelled product while mixing. After 1 h, 200 mL additional methanol was added to the yellow dispersion of the hydrogel (H-Na-PCMTKP-*g*-PAN) to complete the precipitation. The supernatant was decanted after 30 min and 300 mL fresh methanol was then further added to completely de-water the particles for 24 h. The yellow precipitate of the hydrogel (H-Na-PCMTKP-*g*-PAN) was filtered through sintered glass crucible (no. 3) using suction. Thus, the product of the hydrogel, H-Na-PCMTKP-*g*-PAN obtained was thoroughly washed with fresh methanol and finally dried at 60 °C and stored in a vacuum desicator.

Swelling or Absorbency Measurements

In order to measure the swelling or absorbency capacity of the hydrogel, 0.1 g of the saponified Na-PCMTKP-*g*-PAN (*i.e.* H-Na-PCMTKP-*g*-PAN) powder, after passing through 100 mesh (150 μm) sieve, was put into a weighed tea bag. The tea bag then was immersed in 200 mL low conductivity water and allowed to soak for different timings (0.5 to 36 h) at room temperature. The equilibrated swollen gel was then allowed to drain by removing the tea bag from the water and was hung up until no more drops drained (*ca*. 10 min). The bag was then weighed to determine the weight of the swollen gel. By using the swelling or absorbency experimental weights of the hydrogel sample, the values of the swelling ratio (S) of the hydrogel sample were calculated using the following equation:

$$S = \frac{W_s - W_d}{W_d} \tag{6}$$

where W_s and W_d are the weights of the swollen gel and the dry gel, respectively. Thus, the swelling ratio (S) was calculated as grams of water per grams of hydrogel sample (g/g gel). The water absorption capacity was determined three repeats for each case and its average value was reported.

Swelling in Salt Solutions

Absorbency measurements of the H-Na-PCMTKP-*g*-PAN hydrogel sample were also carried out in 0.15 $mol \cdot L^{-1}$ solutions of NaCl, $CaCl_2$ and $AlCl_3$ as well as in Simulated Urine (composition : 0.85 g $CaCl_2 \cdot 2H_2O$, 1.14 g $MgSO_4 \cdot 7H_2O$, 8.20 g NaCl, 20 g urea and 1000 mL low conductivity water) solution[19] for different timings (0.5 h to 36 h) according to the method described above for absorbency measurements in low conductivity water.

FTIR Spectra

FTIR spectra of Na-PCMTKP ($\overline{DS}$ = 0.15), Na-PCMTKP-*g*-PAN (*G* = 413.76%), PAN and the superabsorbent hydrogel H-Na-PCMTKP-*g*-PAN samples were taken in KBr pellets using a Nickolet Impact 400D Fourier Transform Infra Red Spectrophotometer.

Thermogravimetric Analysis (TGA)

The thermal behavior of Na-PCMTKP ($\overline{DS}$ = 0.15), Na-PCMTKP-*g*-PAN (*G* = 413.76%) and PAN has been examined in an inert atmosphere at a heating rate of 10 K/min with the help of a Dupont 951 thermogravimetric analyzer.

Scanning Electron Microscopy (SEM)

A Model ESEM TMP + EDAX, Philips has been used to obtain the micrographs of Na-PCMTKP ($\overline{DS}$ = 0.15), Na-PCMTKP-*g*-PAN (*G* = 413.76%) and the superabsorbent hydrogel, H-Na-PCMTKP-*g*-PAN samples.

RESULTS AND DISCUSSION

Determination of Optimum Reaction Conditions

In the present investigation, various reaction conditions were used to discover the optimum for grafting. The reaction conditions include the amount of Na-PCMTKP, concentrations of initiator (CAN), nitric acid and monomer (AN) as well as temperature and time.

Effect of Amount of Na-PCMTKP

The influence of varying amount of Na-PCMTKP ($\overline{DS}$ = 0.15) (0.5 g to 3.0 g) on *G* as well as *GE* is shown in Fig. 1. It can be seen that both *G* and *GE* increase with an increase in Na-PCMTKP concentration and reaches a maximum value of *G* = 312.28% at the concentration of Na-PCMTKP = 1.0 g. This could be due to availability of more grafting sites with increasing concentration of Na-PCMTKP. As the concentration of Na-PCMTKP further increases, the viscosity of the reaction medium increases, which hinders the movement of free radicals, thereby decreasing the grafting parameter (*G* decreases from 312.28% to 218.39%). Similar results were reported in the literature[20, 21].

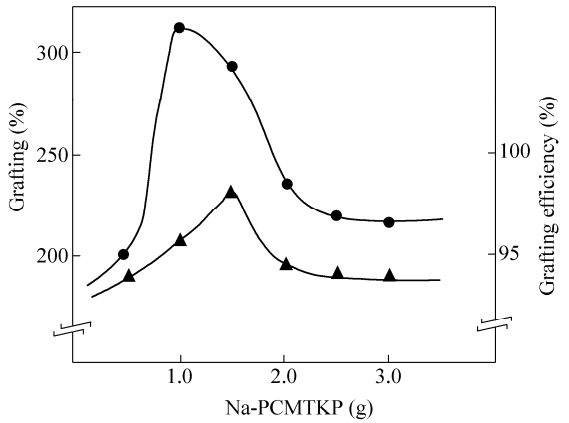

Fig. 1 Effect of amount of Na-PCMTKP on (●) – *G* and (▲) – *GE*

Effect of Initiator Concentration

In Fig. 2, the grafting yields have been plotted as a function of initiator concentration. It is observed that with an increase in ceric ion concentration the value of *G* increases and reaches a maximum value at $[Ce^{4+}]$ = 0.02 mol·L^{-1}, giving rise to 353.62% grafting. Beyond $[Ce^{4+}]$ = 0.02 mol·L^{-1}, the value of *G* decreases. The observed increase in *G*, within the CAN concentration range of 0.0025–0.02 mol·L^{-1}, may be due to the fact that in this concentration range the increasing concentration of ceric-ions results in an increase in the total number of the complex-Na-PCMTKP-ceric ions which decompose to give more active sites. Thus, the activation along the backbone which has taken place is immediately followed by the graft copolymerization of AN onto the backbone. The decrease in *G* as well as *GE* beyond $[Ce^{4+}]$ = 0.02 mol·L^{-1} may be attributed to the formation of homopolymer at the cost of grafting. In addition to this, at higher concentration of the initiator, the ceric ions take part in the termination of growing grafted chains leading to the decrease in the grafting yields. Similar results were reported elsewhere[22, 23].

Effect of Nitric Acid Concentration

Figure 3 represents the dependence of the grafting yields (*G* and *GE*) on the nitric acid concentration. Interestingly, a high value of *G* which is being observed at zero concentration of acid (cf. Fig. 3) is attributed to the fact that even in absence of acid, in an aqueous medium Na-PCMTKP swells to a greater extent which facilitates the availability of the functional groups for grafting. It can be further seen from this figure that there exists an optimum concentration of nitric acid (0.2 mol·L^{-1}) affording maximum percentage of grafting (*i.e.* *G* = 355.22%). Beyond the optimum concentration of acid, the observed decrease in the grafting yields may be attributed to the formation of more and more Ce^{4+} and $[Ce(OH)_3]^{3+}$ species affecting the grafting adversely. Similar results were reported in the literature[24–26].

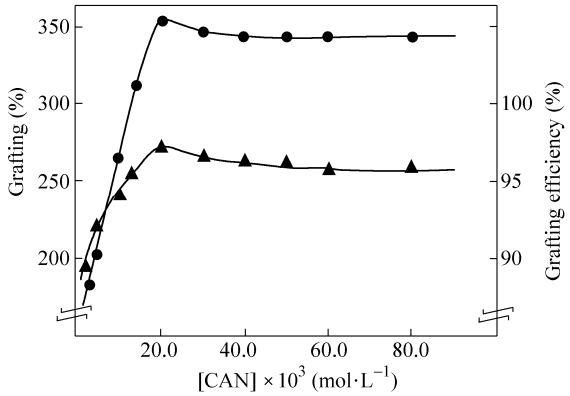

Fig. 2 Effect of ceric ammonium nitrate concentration on (●) – *G* and (▲) – *GE*

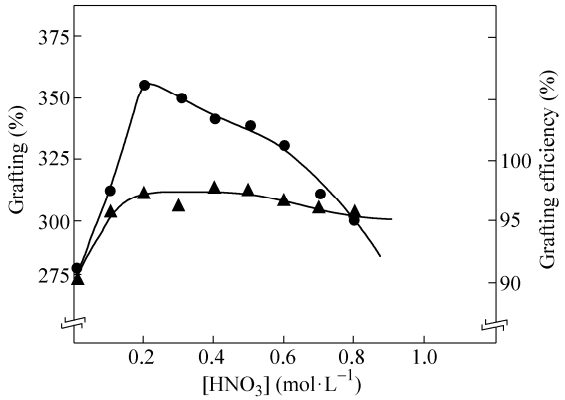

Fig. 3 Effect of nitric acid concentration on (●) – *G* and (▲) – *GE*

Effect of Monomer Concentration

Figure 4 illustrates the influence of monomer (AN) concentration on the grafting yields (*G* and *GE*). The continuous increase in *G* with increasing monomer concentration might be attributed due to accumulation of monomer molecules at the immediate vicinity to the polymeric backbone. Thus, the monomer molecules, which are in the close proximity of reaction sites become acceptors of Na-PCMTKP macroradicals resulting in the enhancement of chain initiation and thereafter themselves become donor of free radicals to neighbouring molecules causing the lowering of termination. However, the observed decrease in grafting efficiency (*GE*) beyond [AN] = 0.222 mol·L^{-1} may be due to the fact that the grafted chains acting as diffusion barriers, which may impede diffusion of monomer into the backbone leading to the poor availability of monomer for grafting thereby resulting in the formation of homopolymer. These observations are also in line with those reported in the literature[22, 27, 28].

Effect of Temperature

In order to examine the influence of temperature, the graft copolymerization was recorded at different temperatures ranging from 15 °C to 55 °C while keeping other reaction parameters constant. From the results (Fig. 5) it becomes evident that the grafting yields (*G* and *GE*) increase with increase in temperature from 15 °C to 40 °C beyond which they decrease. This behavior can be attributed to the increased rate of polymerization at higher temperature. However, after reaching the optimum temperature (40 °C), a further increase in temperature could result in the enhanced mobility of macroradicals which may lead to termination, resulting in the decrease of the grafting yields (cf. Fig. 5). Similar results were reported in the literature[22, 29, 30, 31].

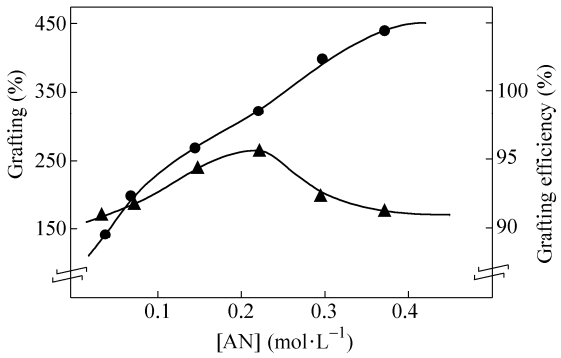

Fig. 4 Effect of acrylonitrile (AN) concentration on (●) – *G* and (▲) – *GE*

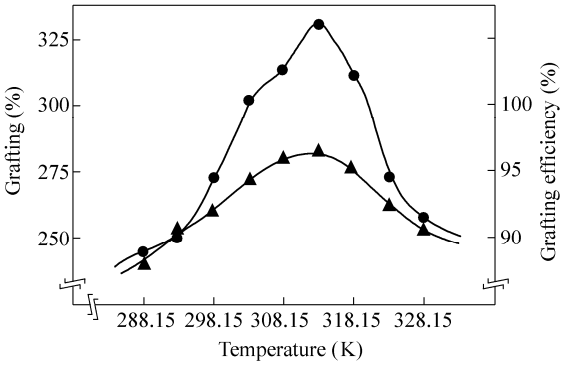

Fig. 5 Influence of temperature on (●) – *G* and (▲) – *GE*

Effect of Reaction Time

The influence of reaction time on the grafting yields is shown in Fig. 6. It can be seen that with the initial increase in time, the percentage grafting increases, reaches an optimum value (312.28%) at 4 h and decreases with further increase in the reaction time. This increase in *G* is due to the increase in the number of grafting sites on the Na-PCMTKP backbone as reaction progresses. But beyond 4 h, the decrease in both the grafting yields is due to the depletion in monomer and initiator concentrations as well as shortage of the available grafting sites. Similar results were reported in the literature[21, 22, 28].

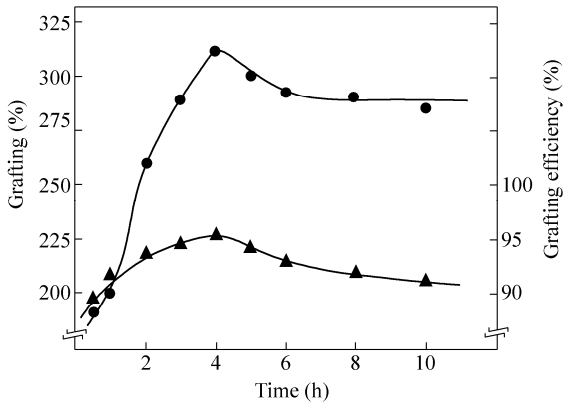

Fig. 6 Influence of reaction time on (●) – *G* and (▲) – *GE*

Thus, from the above discussion the optimal reaction conditions evaluated in the case of graft copolymerization of AN onto Na-PCMTKP ($\overline{DS}$ = 0.15) are: Na-PCMTKP ($\overline{DS}$ = 0.15) = 1.0 g (dry basis), [CAN] = 20×10^{-3} mol·L^{-1}, [HNO_3] = 0.20 mol·L^{-1}, [AN] = 0.222 mol·L^{-1}, reaction time = 4 h, temperature = 40 °C and total volume = 150 mL. At the optimum grafting reaction conditions, the maximum values of the grafting yields achieved are *G* = 413.76%, *GE* = 96.48% and H_p = 3.52%.

Kinetics and Mechanism

The mechanism of free radical graft copolymerization of AN onto Na-PCMTKP ($\overline{DS}$ = 0.15) is expected to proceed according to the scheme, which was proposed earlier by us[23, 29]. Scheme 1 represents the mechanistic pathway for the synthesis of Na-PCMTKP-*g*-PAN. The present experimental results, as tabulated in Tables 1 and 2, have been treated in light of the proposed kinetic scheme and accordingly the plot of R_g versus $[CAN]^{0.5}$ should be linear at lower [CAN]. Such type of typical plot obtained in the present case is shown in Fig. 7 which is found to be linear at lower [CAN], indicating that termination takes place by recombination of double radicals as per Eq. (12) of the kinetic scheme proposed earlier[23, 29]. However, the plot deviates from linearity at higher initiator concentration further indicating that the termination takes place by single radical, as per Eq. (15) of the kinetic scheme proposed earlier[23, 29] leading to the decrease in the rate of graft copolymerization. The effect of the monomer (AN) concentration as well as the initiator (CAN) concentration on the overall rate of polymerization (R_P) as expected on the basis of the relationship derived earlier[23, 29] is also exemplified in Fig. 8.

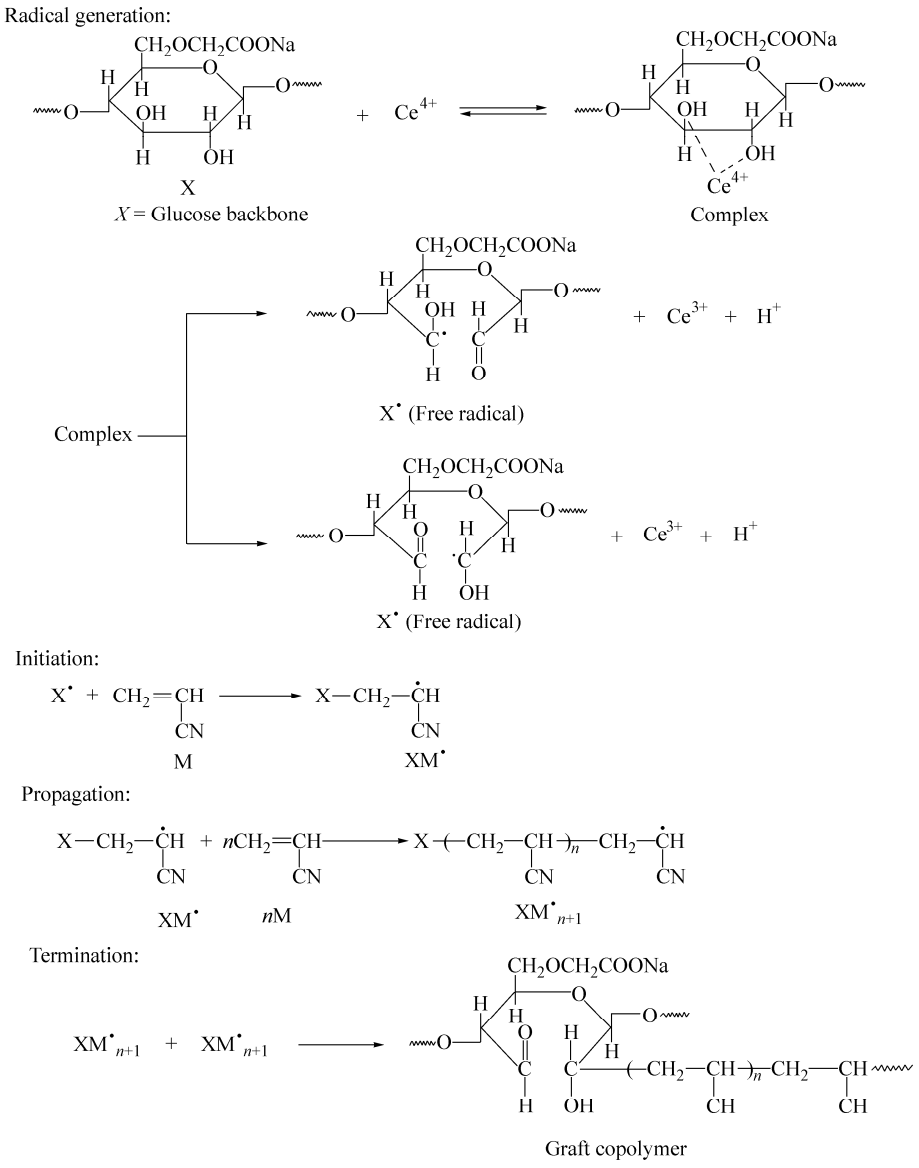

Scheme 1 Mechanistic pathway for the synthesis of Na-PCMTKP-*g*-PAN

As evident, the plots of R_p versus $[M]^2$ and R_p versus $1/[Ce]^{4+}$ are found to be linear in the present case, supporting the proposed kinetic scheme[23, 29].

Table 1. Rates of graft copolymerization (R_g) and polymerization (R_p) for grafting of AN onto Na-PCMTKP ($\overline{DS}$ = 0.15) at various initiator concentrations[a]

$[CAN] \times 10^3$ (mol·L^{-1})	$R_p \times 10^5$ (mol·L^{-1}·s^{-1})	$R_g \times 10^5$ (mol·L^{-1}·s^{-1})
2.5	1.78	1.57
5.0	1.93	1.78
10.0	2.42	2.28
13.0	2.85	2.72
20.0	3.17	3.09
30.0	3.14	3.03
40.0	3.14	3.02
50.0	3.12	3.00
60.0	3.12	2.99
80.0	3.12	2.99

[a] Na-PCMTKP ($\overline{DS}$ = 0.15) = 1.0 g (dry basis); [CAN] = varied as shown; $[HNO_3]$ = 0.10 mol·L^{-1}; [AN] = 0.222 mol·L^{-1}; Time = 4 h; Temperature = 35 °C; Total volume = 150 mL

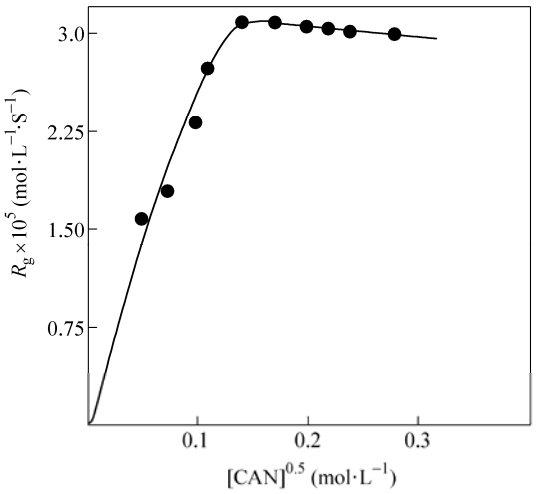

Fig. 7 Plot of R_g versus $[CAN]^{0.5}$

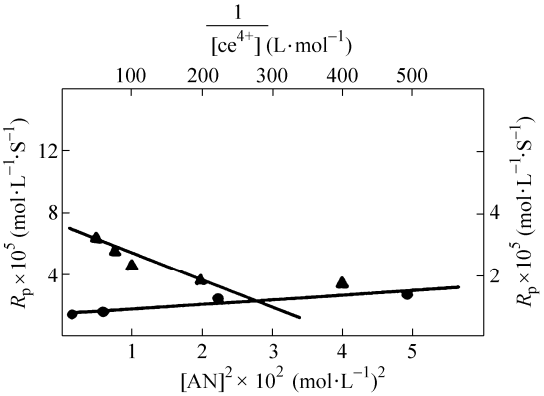

Fig. 8 Plots of R_p versus $[M]^2$ (●) and $1/[Ce]^{4+}$ (▲)

Table 2. Rate of polymerization (R_p) for grafting of AN onto Na-PCMTKP ($\overline{DS}$ = 0.15) at various initiator concentrations[a]

[AN] (mol·L^{-1})	$R_p \times 10^5$ (mol·L^{-1}·s^{-1})
0.037	1.35
0.074	1.88
0.148	2.44
0.222	2.85

[a]Na-PCMTKP ($\overline{DS}$ = 0.15) = 1.0 g (dry basis); [CAN] = 0.013 mol·L^{-1}; [HNO_3] = 0.10 mol·L^{-1}; [AN] = varied as shown; Time = 4 h; Temperature = 35 °C; Total volume = 150 mL

Evidence of Grafting

FTIR-spectra

Figure 9(a) shows the IR spectrum of Na-PCMTKP ($\overline{DS}$ = 0.15). The presence of a very strong and broad absorption band at *ca*. 3433 cm^{-1} is assigned to —OH stretching. Reasonably sharp absorption band at *ca*. 2924 cm^{-1} may be attributed to the —CH stretching. The asymmetric and symmetric vibrations of —COO— moiety are assigned to *ca*. 1641 cm^{-1} and *ca*. 1423 cm^{-1} respectively. This can be attributed to the incorporation of carboxymethyl groups in tamarind kernel powder (TKP).

Spectra (b) and (d) in Fig. 9 represent the IR spectra of Na-PCMTKP-*g*-PAN and PAN (isolated by hydrolysis method) samples, respectively. The spectra of the graft copolymer (Fig. 9b) showed absorption bands of Na-PCMTKP ($\overline{DS}$ = 0.15) as well as an additional band at *ca*. 2245 cm^{-1}, which has been attributed to —C≡N stretching mode, characteristic of the spectra of PAN (Fig. 9d). Thus, the presence of an additional band at *ca*. 2245 cm^{-1} in the graft copolymer (*i.e*. Na-PCMTKP-*g*-PAN) indicates beyond doubt that grafting of AN onto Na-PCMTKP ($\overline{DS}$ = 0.15) has taken place.

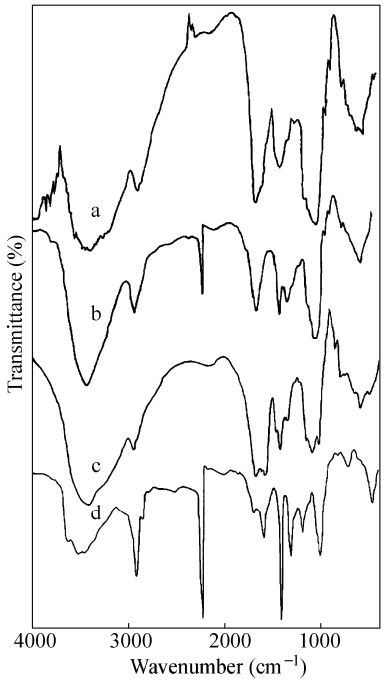

Fig. 9 FTIR spectra of (a) sodium salt of partially carboxymethylated tamarind kernel powder, Na-PCMTKP ($\overline{DS}$ = 0.15), (b) Na-PCMTKP-*g*-PAN (G = 413.76%), (c) the superabsorbent hydrogel, H-Na-PCMTKP-*g*-PAN and (d) polyacrylonitrile (PAN)

Scanning Electron Microscopy (SEM)

The scanning electron micrographs of Na-PCMTKP ($\overline{DS}$ = 0.15) and Na-PCMTKP-*g*-PAN are shown in Figs. 10(a) and 10(b) respectively. In the case of Na-PCMTKP ($\overline{DS}$ = 0.15), the observed surface morphology showing the clustered granular structure is due to its branched structure and interactions of the hydrophilic or ionic groups present onto it. On the other hand after grafting with PAN, a hydrophobic polymer, the surface of the resultant Na-PCMTKP-*g*-PAN (*G* = 413.76%) exhibits contrastingly different morphology (cf. Fig. 10b), compared to that of the Na-PCMTKP ($\overline{DS}$ = 0.15) (Fig. 10a), due to the hydrophobic-hydrophobic interactions taking place between the grafted PAN chains assemble on the surface of the backbone polymer. Thus, the surface evidence supports the grafting of PAN onto the Na-PCMTKP ($\overline{DS}$ = 0.15).

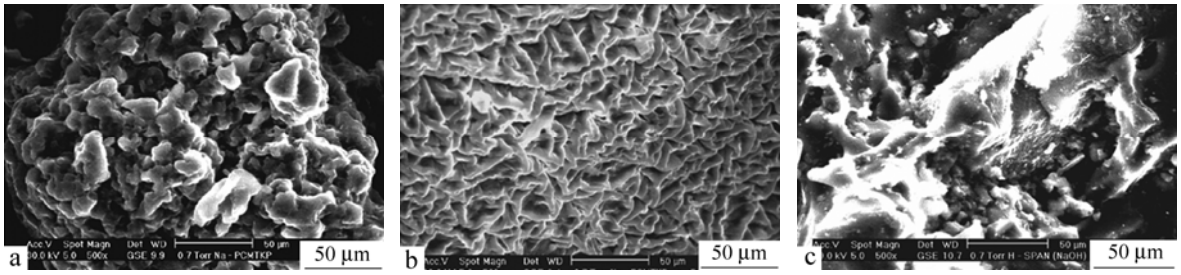

Fig. 10 Scanning electron micrographs of (a) sodium salt of partially carboxymethylated tamarind kernel powder (Na-PCMTKP, $\overline{DS}$ = 0.15), (b) Na-PCMTKP-*g*-PAN (G = 413.76%) and (c) the superabsorbent hydrogel, H-Na-PCMTKP-*g*-PAN

Thermogravimetric Analysis (TGA)

The thermal behavior of Na-PCMTKP ($\overline{DS}$ = 0.15), Na-PCMTKP-*g*-PAN (*G* = 413.76%) and PAN was examined by studying their primary thermograms (Fig. 11) in nitrogen atmosphere at 10 $K \cdot min^{-1}$. As it can be observed that the overall degradation of Na-PCMTKP involves two steps. The sample begins to decompose at about 220 °C and loses its weight very slowly up to 400 °C involving about 57% weight loss. The second decomposition step is immediately followed and marked with a rapid weight loss in the temperature range 400–590 °C during which the sample loses 38% of its weight. The temperatures of maximum rates of weight loss for the first and second decomposition steps are 300 °C and 495 °C respectively. The overall degradation leaves about 5% residue.

The graft copolymer (Na-PCMTKP-*g*-PAN) sample (Fig. 11), involves two steps of degradation. The first step of degradation encompasses the temperature range from 190 °C to 355 °C amounting to a loss of about 24% weight exhibiting maximum rate of weight loss at 305 °C. The second step comprises of 355–720 °C, involving about 68.5% weight loss reaching a maximum at 525 °C. The overall degradation leaves about 7.5% residue.

The overall degradation of PAN (Fig. 11) also comprises of two steps. The sample begins to decompose at 270 °C and loses its original weight up to 500 °C involving about 27% weight loss and exhibiting maximum rate of weight loss at 355 °C. The second decomposition occurs immediately in the temperature range 500°C–780 °C during which the sample loses 60.5% of its weight reaching a maximum rate of weight loss at 665 °C. The observed char yield is 12%.

The values of the temperature characteristics, the integral procedural decomposition temperature (IPDT) and the decomposition temperature (T_D) at every 10% weight loss for Na-PCMTKP ($\overline{DS}$ = 0.15), Na-PCMTKP-*g*-PAN (*G* = 413.36%) and PAN samples are tabulated in Table 3. The examination of IPDT values indicates that the overall thermal stability of Na-PCMTKP has been increased to a greater extent upon grafting of AN onto it. The increased ring formation at higher temperatures may be responsible for the observed higher value of IPDT for the graft copolymer sample compared to that of Na-PCMTKP ($\overline{DS}$ = 0.15)[22]. The value of IPDT for PAN sample is found to be higher than that of the graft copolymer (Na-PCMTKP-*g*-PAN) as well as Na-PCMTKP ($\overline{DS}$ = 0.15) samples.

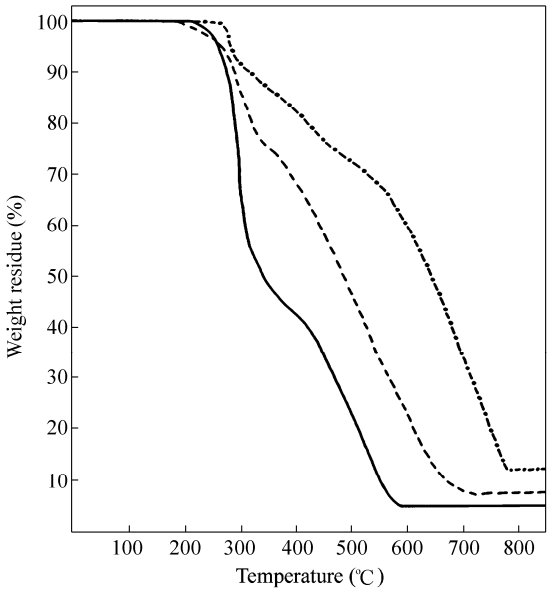

Fig. 11 TG thermograms for (—) Na-PCMTKP ($\overline{DS}$ = 0.15), (-----)Na-PCMTKP-*g*-PAN (G = 413.76%) and (—•—•—) PAN at 10 K·min^{-1}

Table 3. Thermogravimetric analysis data of Na-PCMTKP ($\overline{DS}$ = 0.15), Na-PCMTKP-*g*-PAN (G = 413.76%) and PAN samples

Sample	T_i (°C)(IDT)	T_f (°C) (FDT)	T_{max} (°C)		IPDT [a] (°C)
			Step-1	Step-2	
Na-PCMTKP ($\overline{DS}$ = 0.15)	220	590	300	495	394
Na-PCMTKP-*g*-PAN (G = 413.76%)	190	720	305	525	499
PAN	270	780	355	665	632

Sample	Decomposition temperature (T_D) at every 10% weight loss T_D (°C)								
	10%	20%	30%	40%	50%	60%	70%	80%	90%
Na-PCMTKP ($\overline{DS}$ = 0.15)	275	290	300	315	340	425	470	510	550
Na-PCMTKP-*g*-PAN (G = 413.76%)	300	330	400	450	495	535	575	620	680
PAN	330	430	540	605	650	680	720	750	–

[a] IPDT = A^* ($T_f - T_i$) + T_i, where A^* is the fractional area under the thermogravimetric curve normalized with respect to residual weight.

Thus, the comparison of the results of TGA of Na-PCMTKP ($\overline{DS}$ = 0.15) with that of Na-PCMTKP-*g*-PAN (G = 413.76%) and PAN also provides an additional evidence that the grafting has taken place.

Swelling Behavior of the Superabsorbent Hydrogel, H-Na-PCMTKP-g-PAN

Synthesis and mechanism aspect of the hydrogel

The saponification or alkaline hydrolysis of Na-PCMTKP-*g*-PAN (G = 413.76%) sample was carried out by treating it with aqueous 0.7 mol·L^{-1} sodium hydroxide solution at 90–95 °C. Scheme 2 represents the concise mechanism of crosslinking during conversion of nitrile groups of Na-PCMTKP-*g*-PAN into carboxamide and sodium carboxylate groups for the formation of the superabsorbent hydrogel, H-Na-PCMTKP-*g*-PAN. As per the mechanism of the saponification reaction, in the first step the hydroxide ions abstract hydrogen from the —OH group of Na-PCMTKP substrate leading to the formation of the corresponding alkoxide anions. Then, these Na-PCMTKP alkoxide anions (*i.e.* macroradicals) initiate cross-linking reaction between some adjacent polyacrylonitrile pendant chains which leads to the formation of deep red color intermediate with naphthyridine

cyclic structures, including imine, with evolution of ammonia. This intermediate, then further gets saponified with residual sodium hydroxide solution to produce hydrophilic carboxamide and carboxylate groups. The disappearance of the conjugated system with the formation of the hydrophilic groups was indicated when color of the system changed from red to light yellow. This sharp change in color was used as a marker to halt the alkaline or saponification treatment. In this way, the starting hydrophobic graft copolymer sample *i.e.* Na-PCMTKP-*g*-PAN was converted into a hydrophilic gel *i.e.* superabsorbent hydrogel, H-Na-PCMTKP-*g*-PAN.

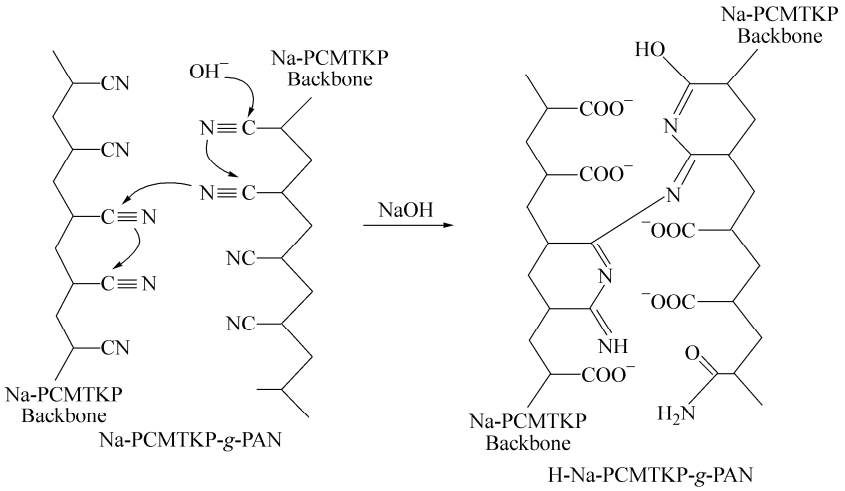

Scheme 2 A concise mechanism for the synthesis of the superabsorbent hydrogel, H-Na-PCMTKP-*g*-PAN

Characterization

FTIR-spectra

IR spectroscopy was used to characterize the superabsorbent hydrogel, H-Na-PCMTKP-*g*-PAN (Fig. 9c). The disappearance of the nitrile sharp peak of Na-PCMTKP-*g*-PAN at *ca*. 2245 cm^{-1}, and appearance of the two distinct bands at *ca*. 1578 cm^{-1} and *ca*. 1409 cm^{-1}, indicating the respective presence of C=O asymmetric stretching and symmetric stretching modes of the carboxylate anions as well as the absorption band appeared at *ca*. 1671 cm^{-1} indicating C=O stretching in carboxamide functional groups are the major proofs for the conversion of the nitrile groups into carboxamide and carboxylate groups after alkaline hydrolysis of the graft copolymer (Na-PCMTKP-*g*-PAN). The presence of these highly hydrophilic groups is the main responsible factor for imparting super swelling behavior of the superabsorbent hydrogel, H-Na-PCMTKP-*g*-PAN.

Scanning electron microscopy (SEM)

Figure 10(c) represents the scanning electron micrograph of the superabsorbent hydrogel, H-Na-PCMTKP-*g*-PAN. The appearance of the pores is regarded to be the regions for the penetration of water into the polymeric network, and ultimately it helps in enhancing the water absorbency of the hydrogel.

Swelling behavior in water and salt solutions

The swelling behavior of the superabsorbent hydrogel could be significantly affected by various factors of the external solutions such as its valences and ionic strength. The presence of ions in the swelling medium has a profound effect on the swelling behavior of the superabsorbent hydrogels. The underlying principle behind the ionic dependence of swelling is well explained by the Donnan equilibrium theory (Scheme 3). According to this theory, the balance between the osmotic pressure of the swelling system and elastic response of the polymeric network controls the extent of swelling. The osmotic pressure results from the difference in concentration of mobile ions between the interior of the hydrogel network and the external solution. The fundamental feature within the hydrogel, bringing about the unequal distribution, in the present case, is the presence of the ionizable, carboxylate groups (anionic sites) attached to the polymeric network.

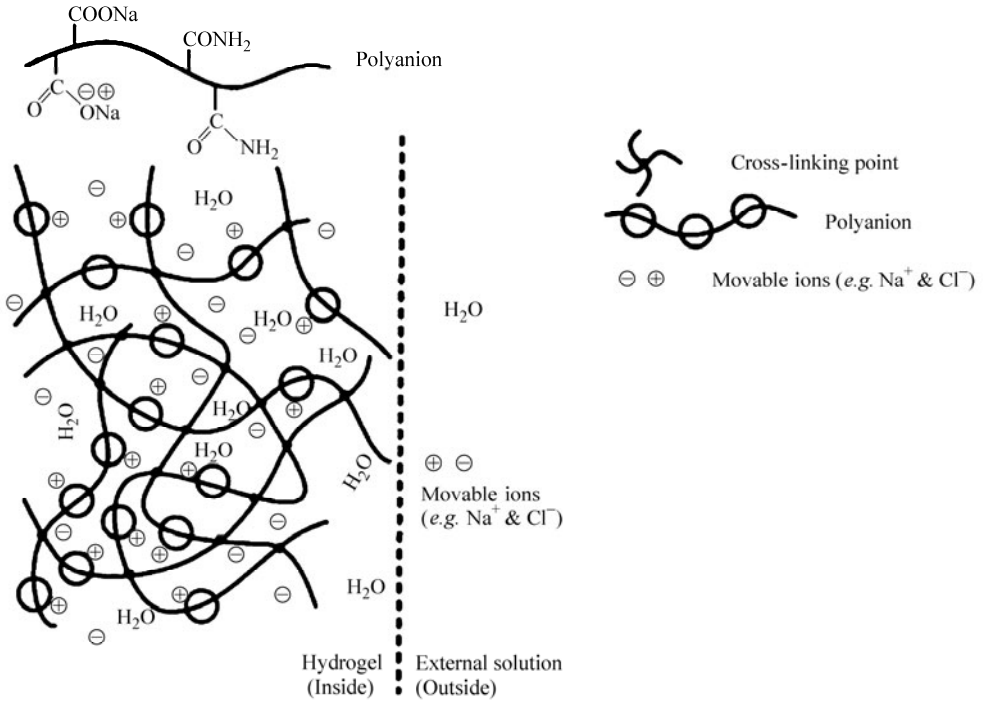

Scheme 3 Representation of swollen anionic superabsorbent hydrogel in equilibrium with electrolyte solution

The results of the swelling ratio values of the superabsorbent hydrogel, H-Na-PCMTKP-*g*-PAN in low conductivity water, 0.15 mol·L^{-1} different salt (NaCl, $CaCl_2$ and $AlCl_3$) solutions and simulated urine [SU][19] are reported in Table 4. The swelling of the anionic hydrogel is found to be increased steadily and continuously with time in the presence of low conductivity water up to 12 h and thereafter it decreases but tends to remain almost constant. However, the swelling ability of the hydrogel in different salt (NaCl, $CaCl_2$ and $AlCl_3$) solutions (0.15 mol·L^{-1}) and in simulated urine solution (0.15 mol·L^{-1}) is found to be decreased at different timings in comparison with the values observed in low conductivity water. This well known phenomenon, which is generally being observed in the swelling of ionic hydrogels[32] is attributed to a "charge screening" effect of the additional counter ions (cations) creating a non-perfect anion-anion electrostatic repulsion, leading to a decreased osmotic (ionic) pressure difference between the hydrogel network and the external solution (Scheme 3). At the swelling equilibrium, the chemical potential of water in the polymer network will be equal to that of the water surrounding to it. However, an addition of a salt to the polymer solution leads to polymer network contraction which may lower the chemical potential of the water surrounding a polymer network. As a result of this, absorbent polymer can not imbibe as much salt water as pure water alone and this is evident from the results of Table 4.

From the results of Table 4, the effect of different cations with a common anion (Cl^-) on the absorbency of the hydrogel, H-Na-PCMTKP-*g*-PAN, can also be explained. The swelling capacity of the hydrogel is found to be decreased with an increase in the charge of the metal cation in the solutions having the same concentration (0.15 mol·L^{-1}). This may be explained by the complexing ability arising from the co-ordination of the multivalent cations with polar and ionic groups present in the hydrogel. Due to the bigger size of the Al^{3+} ions, which may chelate to the nearby polar and ionic groups of the hydrogel but thereby they may hinder the approach of the water molecules leading to the lowering of the water uptake. This "ionic crosslinking" phenomenon mainly occurs at the surface of the particles and as a result, in the present case, the hydrogels are found to be rubbery and very hard to the touch when they swell in Ca^{2+} or Al^{3+} solutions, so that it can not swell well (cf. Table 4). In contrast to this the hydrogel particles are found to be swollen in NaCl solution and water, exhibiting lower gel strength to the touch. Similar results were also reported in the literature[33–36].

Table 4. Swelling ratio (S), (g/g gel) values of the superabsorbent hydrogel, H-Na-PCMTKP-*g*-PAN, in low conductivity water, 0.15 mol·L^{-1} different salt (NaCl, $CaCl_2$ and $AlCl_3$) solutions as well as simulated urine [SU]

Time (h)	Water	NaCl	$CaCl_2$	$AlCl_3$	SU
0.5	59.85 ± 1.70	11.73 ± 1.75	10.11 ± 1.95	4.18 ± 2.25	10.88 ± 1.85
1.0	79.92 ± 1.50	14.32 ± 1.65	13.80 ± 1.85	7.93 ± 2.15	10.92 ± 1.80
1.5	92.20 ± 1.40	19.21 ± 1.55	16.14 ± 1.75	8.32 ± 2.10	13.14 ± 1.75
2.0	110.19 ± 1.30	26.47 ± 1.45	21.95 ± 1.65	11.12 ± 1.95	19.18 ± 1.65
2.5	140.27 ± 1.20	32.17 ± 1.40	22.28 ± 1.60	16.19 ± 1.85	29.43 ± 1.50
3.0	173.18 ± 1.15	46.10 ± 1.35	26.81 ± 1.55	21.13 ± 1.75	40.25 ± 1.45
3.5	182.74 ± 1.10	50.16 ± 1.25	32.43 ± 1.50	27.62 ± 1.70	48.58 ± 1.35
4.0	192.94 ± 1.00	65.86 ± 1.15	52.14 ± 1.45	38.10 ± 1.65	60.40 ± 1.30
8.0	201.54 ± 0.90	66.42 ± 1.10	55.24 ± 1.40	38.00 ± 1.60	62.70 ± 1.25
12.0	247.23 ± 0.65	67.12 ± 1.10	62.78 ± 1.35	42.17 ± 1.55	63.14 ± 1.20
16.0	242.11 ± 0.70	67.53 ± 1.05	62.50 ± 1.30	45.72 ± 1.45	63.52 ± 1.15
20.0	242.14 ± 0.75	67.82 ± 1.04	62.13 ± 1.25	43.17±1.40	65.20 ± 1.12
24.0	241.92 ± 0.60	68.45 ± 1.02	62.16 ± 1.20	43.97 ± 1.30	65.12 ± 1.10
36.0	241.83 ± 0.55	68.13 ± 1.00	62.12 ± 1.15	42.92 ± 1.20	64.63 ± 1.07

Values are recorded as mean ± standard deviations

CONCLUSIONS

In summary, we have reported first time the establishment of the optimum reaction conditions for ceric-induced graft copolymerization of AN onto Na-PCMTKP ($\overline{DS}$ = 0.15) by varying various reaction conditions. The influence of the reaction conditions on grafting yields has been discussed. Under the optimized reaction conditions the maximum percentage of grafting yields achieved are *G* = 413.76% and *GE* = 96.48%. The experimental results have been analyzed in terms of the earlier proposed kinetic scheme and are found to be in good agreement with it. The nitrile groups of Na-PCMTKP-*g*-PAN (*G* = 413.76%) have been completely converted into a mixture of hydrophilic carboxamide and carboxylate groups during alkaline hydrolysis followed by *in situ* cross-linking of the grafted PAN chains. The swelling behavior of the unreported superabsorbent hydrogel, H-Na-PCMPSy-*g*-PAN, has been studied in different swelling media. The results regarding the absorbency measurements of the hydrogel in different swelling media have been successfully explained on the basis of the "charge screening" effect and "ionic cross-linking" phenomenon. The observed retention of about 60 g of water by the hydrogel in the presence of simulated urine and that too within 4 h is good enough to make the hydrogel as potential candidate for personal health care application. FTIR, TGA and SEM techniques have been successfully used to characterize all the products.

REFERENCES

1 Bhattacharya, A., Rawlins, J.W. and Ray, P., Eds. "Polymer Grafting and Crosslinking", Wiley, New Jersey, 2009

2 Peppas, N.A. and Mikes, A.G., "Preparation Method and Structure of Hydrogels" in Hydrogels in Medicine and Pharmacy, CRS press, Boca Raton FL, 1986, Vol. 1

3 Hoffman, A.S., "Intelligent Polymers (in Medicine and Biotechnology)" in Polymeric Materials, Encylopedia Salamone J C Ed. CRC Pres,s Boca Raton FL, 1996, Vol 5, p. 3282

4 Pourjavadi, A. and Zohuriaan-Mehr, M.J., Strach/Strake., 2002, 54(3–4): 140

5 Sinha, V.K., Patel, C.P. and Trivedi, H.C., J. Polym. Mater., 1993, 10: 209

6 Shah, S.B., Patel, B.K., Patel, C.P. and Trivedi, H.C., Starch/Strake., 1992, 44(3): 108

7 Pourjavadi, A., Zohuriaan-Mehr, M.J., Ghasempoori, S.N. and Hossienzadeh, H., J. Appl. Polym. Sci., 2007, 103(2): 877

8 Wang, W. and Wang, A,. Carbohydr. Polym., 2010, 80(4): 1028

9 Mohamadnia, Z., Zohuriaan-Mehr, M.J., Kabiri, K. and Nouri-Razavi, M., J. Polym. Res., 2008, 15(3): 173

10 Tian, D.T., Li, S.R., Liu, X.P., Wang, J.S., Hu, S., Liu, C.M. and Xie, H.Q., J. Appl. Polym. Sci., 2012, 125(4): 2748

11 Gidley, M.J., Lillford, P.J., Rowlands, D.W., Lang, P., Dentini, M., Crescenzi, V., Edwards, M., Fanutti, C. and Grant

Reid, J.S., Carbohydr. Res., 1991, 214(2): 299
12 Kooiman, P., Rev. Trav. Chim. Pays-Bas., 1961, 80: 849
13 Goyal, P., Kumar, V. and Sharma, P., J. Appl. Polym. Sci., 2008, 108(6): 3696
14 Goyal, P., Kumar, V. and Sharma, P., J. Appl. Polym. Sci., 2009, 114(1): 377
15 Sen, G. and Pal, S., Macromol. Symp. 2009, 277(1): 100
16 Vijayakumar, M.T., Rami Reddy, C. and Joseph, K.T., Eur. Polym. J., 1985, 21(4): 415
17 Brockway, C.E. and Seaberg, P.A., J. Polym. Sci. A1, 1967, 5(6): 1313
18 Fanta, G.F., Burr, R.C., Doane, W.M. and Russel, C.R., Starch/Starke., 1978, 30(7): 237
19 Ziderman, II. and Bleayche, J., J. Appl. Polym. Sci., 1986, 32(7): 5791
20 Tripathy, J., Mishra, D.K., Yadav, M. and Behari, K., Carbohydr. Polym., 2010, 79(1): 40
21 Shah, S.B., Patel, C.P. and Trivedi, H.C., Carbohydr. Polym., 1995, 26(1): 61
22 Trivedi, J.H., Kalia, K., Patel, N.K. and Trivedi, H.C., Carbohydr. Polym., 2005, 60(1): 117
23 Shah, S.B., Patel, C.P. and Trivedi, H.C., Die Angewandte Makromol. Chemie., 1994, 214(1): 75
24 Trivedi, J.H., Kalia, K., Patel, N.K. and Trivedi, H.C., J. Appl. Polym. Sci., 2005, 96(5): 1855
25 Dholakia, A., Jivani, J., Trivedi, J.H., Patel, K.H. and Trivedi, H.C., J. Appl. Polym. Sci., 2012, 124(6): 4945
26 Trivedi, J.H., Dholakia, A., Patel, K.H. and Trivedi, H.C., Trends in Carbohydrate Research, 2009, 1(2): 38
27 Vora, R.A., Trivedi, H.C., Patel, C.P. and Trivedi, M.C., J. Appl. Polym. Sci., 1995, 58(9): 1543
28 Yadav, M., Mishra, D.K. and Behari, K., Carbohydr. Polym., 2011, 85(1): 29
29 Trivedi, J.H., Kalia, K., Patel, N.K. and Trivedi, H.C., Polym. Polym. Compos., 2005, 13(3): 301
30 Liu, Y., Zhang, R., Zhang, J., Zhou, W. and Li, S., Iran Polym. J., 2006, 15(12): 935
31 Yadav, M., Sand, A. and Behari, K., Chinese J. Polym. Sci., 2010, 28(5): 673
32 Castel, D., Ricard, A. and Audebert, R., J. Appl. Polym. Sci., 1990, 39(1): 11
33 Zohuriaan-Mehr, M.J. and Pourjavadi, A., J. Polym. Mater., 2003, 20(1): 113
34 Pourjavadi, A. and Mahdavinia, G.R., Turk J. Chem., 2006, 30: 595
35 Xu, S., Cao, L., Wu, R. and Wang, J., J. Appl. Polym. Sci., 2006, 101(3): 1995
36 Pourjavadi, A., Barzegar, Sh. and Mahdavinia, G.R., Carbohydr. Polym., 2006, 66(3): 386